THERMAL RESISTANCE EFFECTS OF CRUD AND OXIDE LAYERS TO THE SAFETY ANALYSIS

JOOSUK LEE, HYEDONG JEONG, YOUNGSEOK BANG
Korea Institute of Nuclear Safety
62 Gwahak-ro, Yusong-gu, Daejeon, 305-338, Republic of Korea
Tel: +82-42-868-0784, Fax: +82-42-868-0045
Email: jslee2@kins.re.kr

ABSTRACT

Influences of crud and zirconium dioxide layers on the LOCA and RIA safety analysis have been investigated. Preliminary models of thermal conductivity and specific heat of crud were developed based on the porous medium assumption. And recently developed oxide conductivity model in KINS was also used. Developed crud models seem to be reasonable, but further improvement is necessary to simulate the experimental results more precisely, especially in a nucleate boiling regime. In a LOCA safety analysis, cladding temperatures were strongly affected by the crud and oxide layers, as expected. And impacts of thermal layers on cladding temperature and surface heat flux were also strong in a RIA safety analysis, but relatively small influences on fuel enthalpy and fuel temperature were identified.

1. Introduction

Thermal resistance of crud and zirconium dioxide (ZrO_2) layers that were formed on zirconium alloy cladding surface during normal operation of LWR plants was not fully taken into account in the design basis accidents safety analysis such as a loss-of-coolant accident (LOCA) and reactivity-initiated accident (RIA). This is because the limiting fuel burnup is chosen as a beginning of life fuel condition in a LOCA safety analysis, and approved thermal-hydraulics computer codes also have some limitations on simulation of such layers. But the thickness of zirconium oxide layer, which was formed during normal operation, has reached about 60~80 μm at the end of licensing fuel burnup. And sufficient amount of crud buildup can take place on the cladding surface, for example due to the replacement of steam generator in primary coolant circuit in PWR. These were evidenced by several crud-induced power shift events.

Oxide and crud layers formed on cladding surface will behavior as a thermal barrier due to their low thermal conductivity. And apparently it will increase the stored energy during steady-state operation. And heat conduction from fuel to coolant will be inhibited during transient. But unfortunately, robust thermal property models of those layers were not available. For example, thermal conductivity of ZrO_2 showed some differences between well-known FRAPCON and MATPRO models [1]. And, thermal conductivity and specific heat of crud were not successfully developed yet based on the experimental evidences.

In this paper, simple models of the thermal conductivity and specific heat of crud were developed. And recently developed thermal conductivity model of ZrO_2 was used. Impacts of these models on the LOCA and RIA safety analysis have been assessed.

2. Analysis Details

2.1 Crud models

It is known that the crud is a porous medium that is composed of solid phase oxides and liquid water. And if temperature inside of crud reaches the boiling point, the liquid water will be replaced by the mixture of saturated water and gaseous steam. And if temperature exceeds the boiling point, the mixture will be replaced by super-heated steam. In these phenomenological perspectives, following assumptions were made for the model development.

- Solid phase crud is composed of three kinds of oxide such as NiO, $NiFe_2O_4$ and Fe_3O_4 with the volume fraction of 0.15, 0.75 and 0.1, respectively. These oxides are homogeneously

mixed. Thermal properties (thermal conductivity and specific heat) of each oxide species utilized in this study are listed in Table 1.

- Average volume fraction of liquid water inside of crud can be varied as a function of porosity, p. If p equals zero, it means the crud is completely solid. And the given porosity, the volume fraction of solid crud varied linearly from +0.1(bottom surface) to -0.1(top surface) with respect to the given porosity.
- In a subcooled and nucleate boiling regime, if the temperature of crud exceeds the saturation temperature of water, it assumed that 10 vol. % of steam is encapsulated in liquid crud. And the temperature of steam and liquid water is set to +0.1K above and -0.1K below the saturation temperature, respectively.
- When the surface heat flux exceeds the critical heat flux then boiling regime entered into the transition and film boiling, super-heated steam occupies inside of crud completely.
- There is no directionality between solid phase oxides and liquid (or steam, or mixture) water.

Based on the above assumptions, thermal conductivity of crud(k_{crud}) can be calculated by the following relationships.

$$k_{crud} = (0.5/k_{crud\_max} + 0.5/ k_{crud\_min})^{-1} \quad (1)$$

$$k_{crud\_max} = (1-p)\, k_s + p\, k_w \quad (2)$$

$$k_{crud\_min} = ((1-p) / k_s + p / k_w)^{-1} \quad (3)$$

$$k_s = 0.15k_{NiO} + 0.75\, k_{NiFe2O4} + 0.1\, k_{Fe3O4} \quad (4)$$

where,

k_{crud} = crud thermal conductivity
k_{crud_max} = maximum thermal conductivity (parallel case)
k_{crud_min} = minimum thermal conductivity (serial case)
k_s, k_w = thermal conductivity of solid oxides and liquid water
k_{NiO}, $k_{NiFe2O4}$, k_{Fe3O4} = thermal conductivity of NiO, $NiFe_2O_4$ and Fe_3O_4
p = volume fraction of liquid water

Specific heat of crud ($C_{P\,crud}$) also can be calculated based on the following relationships.

$$C_{P\,crud} = ((1-p)\, \rho_s C_{Ps} + p\, \rho_w C_{Pw})/\rho_{ave} \quad (5)$$

$$\rho_s C_{Ps} = 0.15\, \rho_{NiO} C_{P\,NiO}, + 0.75\, \rho_{NiFe2O4} C_{P\,NiFe2O4}, + 0.1\, \rho_{Fe3O4} C_{P\,Fe3O4} \quad (6)$$

where,

$C_{P\,crud}$ = specific heat of crud
C_{Ps}, C_{Pw} = specific heat of solid oxides and liquid water
$C_{P\,NiO}$, $C_{P\,NiFe2O4}$, $C_{P\,Fe3O4}$ = specific heat of NiO, $NiFe_2O_4$ and Fe_3O_4
ρ_{NiO}, $\rho_{NiFe2O4}$, ρ_{Fe3O4} = density of NiO, $NiFe_2O_4$ and Fe_3O_4
ρ_s, ρ_w, ρ_{ave} = density of solid, liquid and average density

Tab 1 Thermal conductivity and specific heat of NiO, $NiFe_2O_4$ and Fe_3O_4

	Thermal conductivity, W/m-k	Specific heat, J/kg-K
NiO	$-5.602\times10^{-9}T^3 + 2.435\times10^{-5}T^2 - 0.03543T+21.658$ [2]	R.J Radwanska and Z. Ropka [3]
$NiFe_2O_4$	$1/(4.3711\times10^{-4} + 2.7512\times10^{-2}T)$ [4]	$-1.2057+(1.1411\cdot10^{2})T - (2.4950\cdot10^{5})T^2+(2.4611\cdot10^{8})T^3 - (8.8726\cdot10^{12})T^4$ (298<T<823) [4] $-6.5674+(3.2540\cdot10^{2})T - (5.0578\cdot10^{5})T^2+(3.3300\cdot10^{8})T^3 -(7.9139\cdot10^{12})T^4$ (923<T<1373) [4]
Fe_3O_4	Yasuo and Keiji Naito [5]	Chase [6]

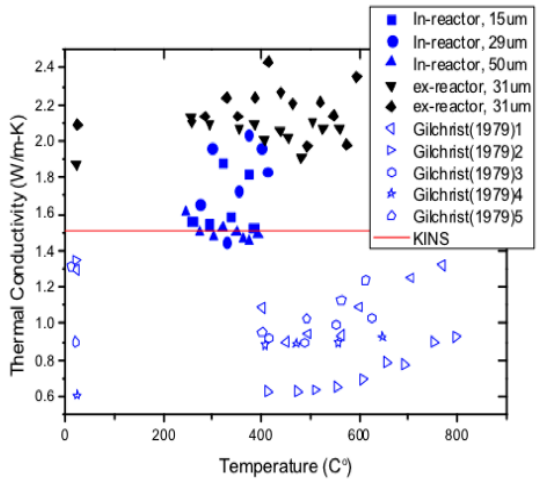

Fig 1. Considered thermal conductivity data of ZrO_2 for the development of conductivity model in KINS [10].

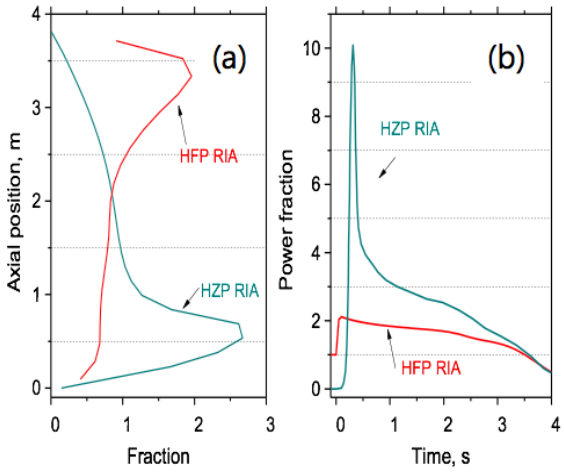

Fig 2. (a) Applied imaginary axial power profiles and (b) applied power pulses for HZP and HFP RIA safety analysis [14].

2.2 Oxide models

Several models of thermal conductivity of ZrO_2 are available. But they showed some differences. For example, the model used in FRAPCON showed about ~ 2W/m-K, but MATPRO model gave about ~1W/m-K, within concerned temperature ranges [1]. This comes from the different experimental data used for model develpment. FRAPCON model was developed based on the Kingery (1954) data [2]. But MATPRO model was adjusted by Gilchrist (1976) data [7]. It was known that Kingery (1954) produced the data by using a zero-porosity specimen, and Gilchrist (1976) data had uncertainty on measuring ZrO_2 thickness. Recently, authors have investigated the thermal conductivity of ZrO_2, and proposed thermal conductivity model by using Gilchrist (1979) and Stehle et. al. (1984) data [8,9]. Fig. 2 shows the data and proposed model. Proposed thermal conductivity is a constant value of 1.51 W/m-K with applicable temperature ranges from room temperature to ~1600K. Lower bound of conductivity is 0.61 W/m-K within 95% probability and 95% confidence level.

On specific heat of ZrO_2, there are no known issues and its impacts on safety analysis are reletavely small. Thus MATPRO model is used in this study.

3. Safety analysis conditions

Impacts of crud and oxide layers to the LOCA and RIA safety analysis have been assessed by using FRAPTRAN-2.0KS computer code. FRAPTRAN-2.0KS is a modified version of FRAPTRAN-2.0 [11] in KINS for the implementation of crud and oxide layer. For the assessment of effective thermal conductivity and specific heat of crud, five evenly spaced radial nodes were allocated in the crud layer. Considered thickness of crud was 30 μm.

APR1400 PWR plant with 16x16 ZIRLO cladding fuel was used for safety analysis. Design parameters of fuel rod, operating conditions, and base irradiation power history were obtained from Topical Report [12]. Initiation of LOCA and RIA was supposed to occur at 30MWd/kgU fuel burnup. Initial condition of fuel rod before accident at that burnup was calculated by FRAPCON-4.0 code [13]. Best-estimated maximum oxide thickness at that burnup was 18.8 μm.

Thermal-hydrauclic boundary conditions such as heat transfer coefficient, pressure and temperature for a LOCA period were obtained from APR1400 LBLOCA analysis. Detailed information on the analysis can be found in authors' previous work [10].

Hot zero power (HZP) and hot full power (HFP) RIA were analyzed in APR1400 plant also. Applied power evolutions are shown in Fig. 2. Single top and bottom skewed imaginary axial power profiles were used for HFP and HZP, respectively. Local peak linear heat rate before HFP RIA was set to 14.7 kW/ft. Total injected energy at the axial peak node from 0 to 4 s was

272.3 cal/g and 131.5 cal/g for HZP and HFP RIA, respectively.
For the sensitivity study of crud oxide layers, three different cases were considered. First is do not consider any layers of crud and oxide. It's called as 'without' condition. Second is factorizing the oxide and crud layer as 18.8 μm and 30 μm, respectively, with a best-estimate thermal conductivity. It's called as 'base'. Third is imposing lower bounds of conductivity in 'base' case condition. It's called as 'conservative'. Imposed oxide conductivity was 0.61 W/m-K, and crud conductivity was reduced 20 % with respect to base case.

4. Results and discussion

4.1 Thermal properties of crud

Assessed effective thermal conductivity of crud is shown in Fig 3(a). Crud conductivity was affected by the temperature and porosity. At 561K with the porosity of 0.4, the conductivity was 1.08 W/m-K. And as temperature elevated it reduced until reaching at ~0.91 W/m-K. As temperature increased further, conductivity reduced abruptly to ~0.35 W/m-K. This suddern drop is caused by the intrusion of superheated steam into the crud by the boiling regime change. Once the superheated steam occupied in the crud completely, the conductivity was insensitive to further temperature increase. Conductivity is also affected by the porosity. As the porosity changed from 0.4 to 0.7, it reduced from 1.08 to 0.81 W/m-K at 561K. This reduction is attributed to the increased water volume in the crud. Water has lower thermal conductivity than the solid oxides.
The currently assessed conductivites are well within the experimentally measured ones. It was reported that the conductivity in a full boiling condition was ranging from 0.519 to 1.39 W/m-K [15]. But it is also known that the conductivity where sub-cooled nucleated boiling initiated is as high as 6.1 W/m-K [15]. This suggests the initiation of boiling has important roles in heat conduction, probably enhance heat transfer. Further study is necessary for improving the model.
Fig. 3(b) shows the assessed specific heat of crud. Specific heat was also varied with temperature and porosity. At 561K with porosity of 0.4, the specific heat was 1.17 J/g-K. And it rised up to the temperature of 617K. Then it reduced until reaching the saturated value of ~1.0 J/g-K. And with further temperature increase it droped to ~0.91 J/g-K. Specific heat is also affected by the porosity. As the porosity increased, it resulted in high specific heat because the water has higher specific heat than the oxides. For example, as can be seen in Fig 3(b), when the porosity changed from 0.4 to 0.7 at 561K, it increased from 1.17 to 1.87 J/g-K. Assessed specific heat seems to be reasonable, but experimental evidences are necessary for validation of the model.

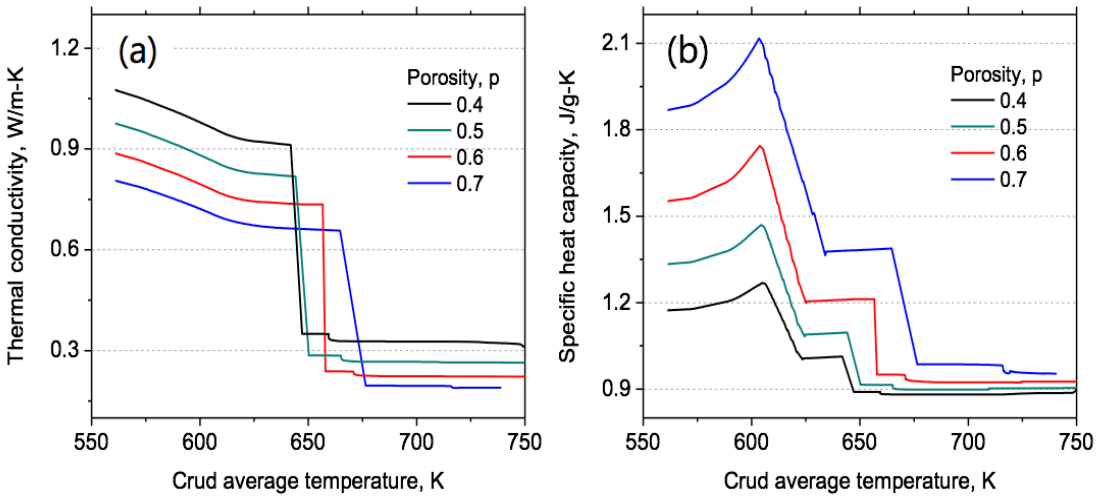

Fig 3. Changes of (a) effective thermal conductivity and (b) specific heat of crud as a function of temperature and porosity at 15.5 MPa coolant pressure and 30 μm thickness of crud.

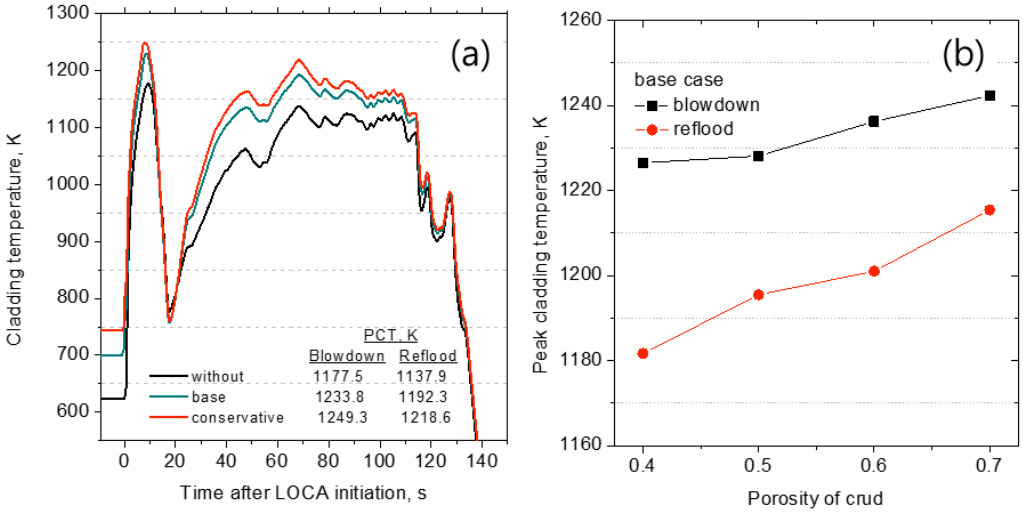

Fig 4. (a) Changes of cladding temperature in APR1400 LBLOCA with consideration of thermal layers of crud and oxide. Crud thickness is 30 μm with porosity of 0.6. (b) PCT changes with porosity of crud in 'base' condition.

4.2 LOCA safety analysis

Fig. 4(a) shows the changes of cladding temperature in APR1400 LBLOCA with factorizing the oxide and crud thermal layers. When the layers were not considered, shown as 'without,' the peak cladding temperature (PCT) observed at blowdown and reflood phase was 1177.5 K and 1137.9 K, respectively. But as the layers were factorized with a normal condition, called as 'base', the PCT rise was 56.3 K and 54.4 K in blowdown and reflood period, respectively. If lower bound thermal conductivities were imposed on the layers, called as a 'conservative', PCT rise was 73.8 K and 80.7 K. These results indicate that the cladding temperatures in LOCA safety analysis are significantly affected by the presence of thermal layers of crud and oxide, and their effects can be prolonged up to the reflood phase. Cladding temperatures also influenced by the porosity fraction in the crud. Fig. 4(b) shows the changes of blowdown and reflood PCT. As the fraction changed from 0.4 to 0.7, blowdown and reflood PCT increased about 16 K and 34 K, reslectively.

4.3 RIA safety analysis

4.3.1 HZP condition

Fig 5 shows the fuel performance change with the modeling of crud and oxide layers in HZP RIA safety analysis. Fig 5(a) and (b) shows an evolution of fuel enthalpy and fuel centerline temperature. In 'base' and 'conservative' condition, changes of peak enthalpy with respect to 'without' case are 6.2 cal/g and 9.0 cal/g, respectively. But fuel centerline temperatures are almost same. This means the influence of the layers on the enthalpy and fuel temperature is relatively small.

Evolution of cladding temperature and surface heat flux were different after modeling of the layers, as shown in Fig 5(c) and (d). Peak cladding temperature in 'base' and 'conservative' condition was 761.3 K and 815.8 K, respectively. This is about 87.8 K and 142.3 K higher than the 'without' condition. As expected, surface heat flux was somewhat reduced due to the thermal resistance.

4.3.2 HFP condition

Fig 6 shows the fuel performance change in HFP RIA condition. Fig 6(a) and (b) shows evolution of fuel enthalpy and fuel centerline temperature. After modeling the thermal layers, fuel enthalpy rise can be found from the initial. And peak fuel enthalpy rise in 'base' and 'conservative' condition with respect to 'without' case is 3.8 cal/g and 9.5 cal/g, respectively.

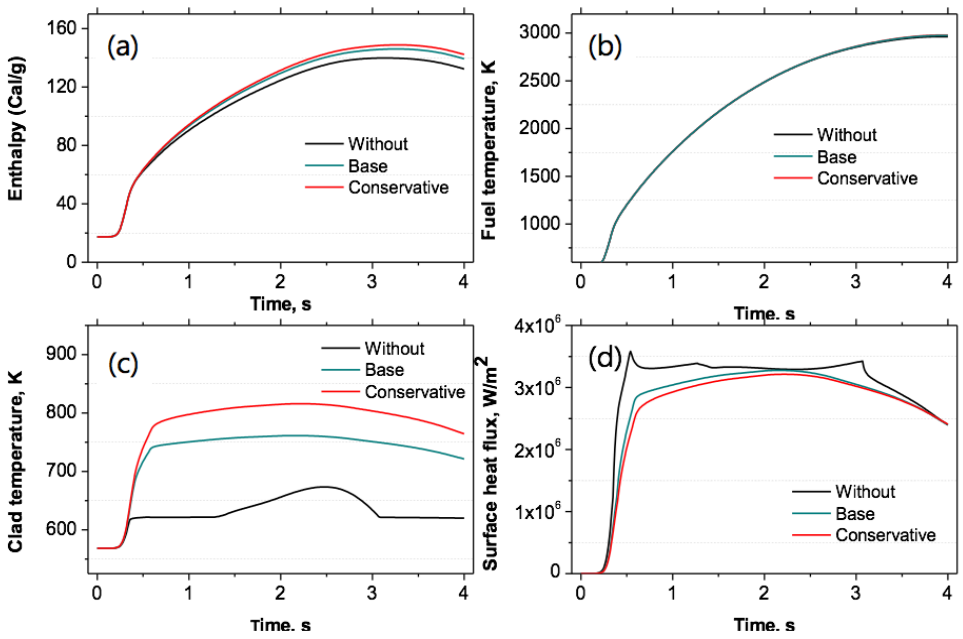

Fig 5. Fuel performance evolution of (a) enthalpy, (b) fuel centreline temperature, (c) cladding temperature, and (d) surface heat flux at hot zero power (HZP) RIA. Crud thickness is 30 μm with porosity of 0.6. Oxide thickness at hot node is 8.4 μm.

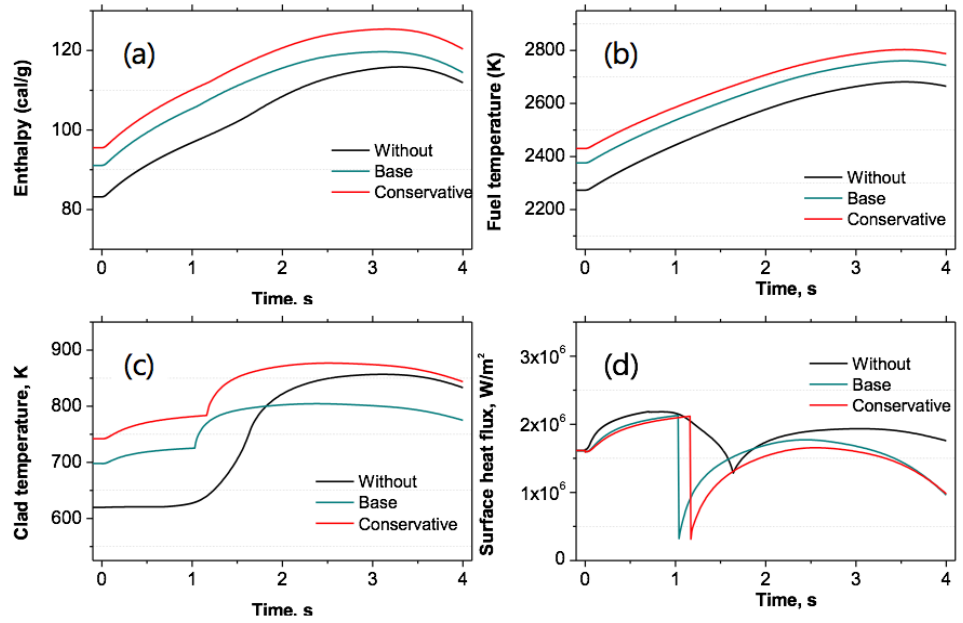

Fig 6. Fuel performance evolution of (a) enthalpy, (b) fuel centreline temperature, (c) cladding temperature, and (d) surface heat flux at hot full power (HFP) RIA. Crud thickness is 30 μm with porosity of 0.6. Oxide thickness at hot node is 18.8 μm.

Behaviors of fuel centerline temperature are similar with the enthalpy evolution. The peak centerline temperature rise in 'base' and 'conservative' condition is about 79.5 K and 121.8 K, respectively. These results reveal that the affected peak fuel enthalpy in HZP and HFP RIA is similar by the modeling of the layers.

Fig 6(c) shows evolution of cladding temperature, and it is strongly affected by the layers. Interestingly thermal layers did not always induce higher cladding temperature during the transient. About 1.8 s after accident initiation, cladding temperature in 'base' condition is lower than the 'without' case. But 'conservative' condition gave always the higher cladding temperature than the others. Evolution of surface heat flux was shown in Fig 6(d). Modeling of thermal layers has induced lower surface hat flux and abrupt drop of heat flux can be found

during transient. These behaviors are related to the boiling regime change combined with thermal resistance effects of the layers.

5. Summary

Preliminary thermal property models of crud and oxide layers were developed. And impacts of these on LOCA and RIA safety analysis were assessed by using FRAPTRAN-2.0KS fuel performance code. Following results can be found.

- Developed models of thermal conductivity and specific heat seem to be reasonable. But more investigation, especially for the heat transfer in nucleate boiling regime will be necessary
- In LOCA safety analysis, cladding temperatures are strongly affected by the thermal layers of crud and oxide.
- In RIA safety analysis, impacts of the crud and oxide layer on fuel enthalpy and fuel temperature are relatively small. But cladding temperature and surface heat flux are affected strongly.

Acknowledgement

This work was supported by the Nuclear Safety Research Program through the Korea Foundation Of Nuclear Safety (KOFONS), granted financial resource from the Nuclear Safety and Security Commission (NSSC), Republic of Korea (No. 1805004-0118-SB110)

References

[1] W.G. Luscher et. al., "Material Property Correlations: Comparison between FRAPCON-3.4, FRAPTRAN-1.4, and MATPRO", NUREG/CR-7024, PNNL-19417, 2011

[2] Kingery, Francl, Coble, Vasilos, J. Am. Ceram. Soc. 37(2) 107-111, 1954.

[3] R.J. Radwanski, and Z. Ropka, "Specific Heat and the Ground State of NiO", ACTA PHYSICA POLONICA A No.1, Vol. 114, 2008.

[4] A.T. Nelson et. al., Thermal Expansion, Heat Capacity and Thermal Conductivity of Nickel Ferrite ($NiFe_2O_4$), Journal of the American Ceramic Society, MIT open access article, 2013.

[5] Yasuo Noda and Keiji Naito, "The Thermal Conductivity and Diffusivity of $MnxFe_3$-xO_4 ($0<x<1.5$) from 200 to 700 K, NETSUSOKUTEI 5(1) 11-18, 1978.

[6] Chase, M.W., Jr., NIST-JANAF Themochemical Tables, Fourth Edition, J. Phys. Chem. Ref. Data, Monograph 9, 1998.

[7] Gilchrist K.E., Thermal Property Measurements on Zircaloy-2 and Associated Oxide Layers Up To 1200℃, Journal of Nuclear Materials, 62, pp.257-264, 1976.

[8] Gilchrist K.E., Thermal Conductivity of Oxide Deposited on Zircaloy Fuel Tube Material – A continuation of Previous Work, Journal of Nuclear Materials, 82, pp.193-194, 1979.

[9] Stehle, H. et al., Characterization of ZrO_2 Films Formed In-Reactor and Ex-Reactor to Study the Factors Contributing to the In-Reactor Waterside Corrosion of Zircaloy, ASTM STP824, 1984.

[10] Y.S. Bang, H.D. Heong, "Development of Thermal Conductivity Model of Cladding Oxide Layer and Impact on LOCA", KINS/RR-1975, 2018.

[11] K.J. Geelhood et. al., "FRAPTRAN-2.0: A Computer Code for the Transient Analysis of Oxide Fuel Rods", May 2016, PNNL-19400, Vol.1. Rev2.

[12] PLUS7 Fuel Design and Safety Evaluation for Korean Standard Nuclear Power Plants, Porperity, KNF-TR-DMR-04001/N/A Rev.0, 2006.

[13] K.J. Geelhood et. al., "FRAPCON-4.0: A Computer Code for the Calculation of Steady-State, Thermal-Mechanical Behavior of Oxide Fuel Rods for High Burnup", PNNL-19418, Vol.1. Rev.2, September 2015.

[14] APR1400 Design Control Document TIER2, Wed-based ADAMS, "https://www.nrc.gov/docs/ML1500/ML15006A054.pdf"

[15] J. Deshon, "Simulated Fuel Crud Thermal Conductivity Measurements Under Pressurized Water Reactor Conditions", EPRI, Palo Alto, CA: 2011. 1022896.